

A discrete model of water with two distinct glassy phases

A. PAGNANI^{1,2} and M. PRETTI³

¹ *HuGeF Torino - Via Nizza 52, I-10126 Torino (Italy)*

² *CMP Politecnico di Torino - Corso Duca degli Abruzzi 24, I-10129 Torino (Italy)*

³ *CNR-ISC and CNISM, Dip.to di Fisica, Politecnico di Torino - Corso Duca degli Abruzzi 24, I-10129 Torino (Italy)*

PACS 64.70.qd – Thermodynamics and statistical mechanics

PACS 64.70.P– – Glass transitions of specific systems

PACS 65.20.Jk – Studies of thermodynamic properties of specific liquids

Abstract. - We investigate a minimal model for non-crystalline water, defined on a Husimi lattice. The peculiar random-regular nature of the lattice is meant to account for the formation of a random 4-coordinated hydrogen-bond network. The model turns out to be consistent with most thermodynamic anomalies observed in liquid and supercooled-liquid water. Furthermore, the model exhibits two glassy phases with different densities, which can coexist at a first-order transition. The onset of a complex free-energy landscape, characterized by an exponentially large number of metastable minima, is pointed out by the cavity method, at the level of 1-step replica symmetry breaking.

Introduction. – In the last decade, there have been several attempts at describing structural glasses by means of simple lattice models, in the analytical framework of random-regular (Bethe or Husimi) lattices [1–5]. For these models, the cavity method generally predicts a discontinuous replica-symmetry breaking, *i.e.*, a sudden emergence of an exponentially large number of metastable free-energy minima. On the other hand, great interest has been attracted by polyamorphism (*i.e.*, the existence of different glass forms of the same substance) [6], both because of the relative novelty of the phenomenon (first discovered for water in 1985 [7]) and because of its relationship with the popular “second critical point” conjecture, put forward by Stanley and coworkers [8] to explain water anomalies [9].

Lattice models have long been used for investigating water [10–22]. In some recent papers, coauthored by one of us [21, 22], it has been shown that a first-order (quasi-chemical) approximation [23] on a tetrahedral cluster is extremely effective to compute the phase diagram and the thermodynamic properties of a special class of water-like models, derived from the early Bell model [10]. These models, defined on the (regular) body-centered cubic (bcc) lattice, do not contain a mechanism capable of inducing glassy behavior, so that they exhibit only crystalline (ice-like) phases at low temperature.

The present letter is motivated by the following observations. i) For a generic lattice model, the aforementioned quasi-chemical approximation, with a given choice of the

associated cluster, coincides with the exact solution of a corresponding model, defined on a Husimi lattice made up of clusters of the same type [23, 24], under the hypothesis of replica symmetry [25, 26]. As a consequence, we can define suitable Husimi lattice models, whose high-temperature behavior turns out to be very similar to that of the original water-like bcc-lattice models. ii) It is known from experiments that directional correlation of hydrogen bonds in real water is almost completely lost after the second consecutive bond (see [27] and references therein). The random nature of a Husimi lattice can roughly describe a similar scenario (this was not possible on a regular lattice). iii) We expect that the resulting frustration might hamper the onset of ice-like order, allowing for the possibility of glassy behavior at low temperature. Such a possibility can be easily investigated by the cavity method [25].

Concerning point i), let us remark the nontrivial difference between a Husimi *tree* (which is, a system with a boundary) and a Husimi *lattice* (which is, a system without a boundary, in which all sites have the same coordination number). The latter system locally exhibits the same tree-like structure as the former, but contains loops on a larger scale [25]. The two systems may be considered equivalent as long as the frustration arising from the presence of loops is not strong enough to induce replica-symmetry breaking (*i.e.*, glassy behavior).

The main finding of this work is a *Husimi lattice* model predicting two different glassy phases, which we are led to

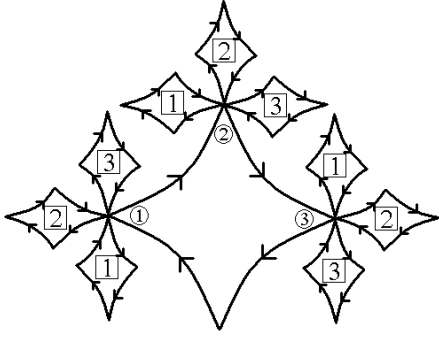


Fig. 1: Portion of the Husimi lattice. Each site is connected to 4 plaquettes. The bottom site, connected only to the central plaquette, gives a pictorial view of the “cavity bias” or “message” concept (see the text).

identify with the low- and high-density amorphous (LDA, HDA) ices, observed experimentally [6, 9]. This model provides interesting insights about the controversial nature of water polyamorphism and, more in general, the metastable phase diagram of water [9].

The model. — We consider a Husimi lattice made up of *oriented* plaquettes of 4 sites, as shown in fig. 1. Each site i (characterized by a configuration variable x_i) may be empty ($x_i = 0$) or occupied by a water molecule, in 2 possible configurations ($x_i = 1, 2$). Each water molecule possesses four equivalent bonding arms, which can point toward nearest neighbor sites, and may be either concordant ($x_i = 1$) or discordant ($x_i = 2$) with edge orientations. An attractive potential energy $-\epsilon < 0$ is assigned to any pair of nearest-neighbor occupied sites. This is the ordinary van der Waals contribution. A hydrogen bond is formed, yielding an extra energy $-\eta < 0$, whenever two nearest-neighbor molecules point an arm toward each other, with no distinction between donors and acceptors (more precisely, a bond is formed on an edge oriented from i to j iff $x_i = 1$ and $x_j = 2$). The hydrogen bond may be weakened by the presence of extra molecules in the same plaquette, namely, each extra molecule gives rise to an energy penalty $\eta c/2$, with $c \in]0, 1[$. The hamiltonian of the system can be written as a sum over plaquettes

$$\mathcal{H} = \sum_{\langle i,j,k,l \rangle} h_{x_i, x_j, x_k, x_l}, \quad (1)$$

where site indices i, j, k, l are enumerated according to the plaquette orientation. The elementary contribution $h_{x,y,z,w}$ (“plaquette energy”) can be written as

$$h_{x,y,z,w} = u_{x,y,z,w} + u_{y,z,w,x} + u_{z,w,x,y} + u_{w,x,y,z}, \quad (2)$$

where

$$u_{x,y,z,w} = -\mu \frac{n_x}{4} - \epsilon n_x n_y - \eta b_{x,y} \left(1 - c \frac{n_z + n_w}{2} \right), \quad (3)$$

n_x is an “occupation function” ($n_x = 0$ if $x = 0$; $n_x = 1$ otherwise), $b_{x,y}$ is a “bond function” ($b_{x,y} = 1$ if $x = 1$ and

$y = 2$; $b_{x,y} = 0$ otherwise), and μ is the chemical potential (we study the grand-canonical ensemble). Looking at eq. (2), one immediately realizes that the plaquette energy is invariant under circular permutations of the configuration variables. As a consequence, the full hamiltonian (1) is unaffected by the choice of the “first site” i in each plaquette.

For the sake of brevity, we have given only a formal description of the model. Indeed, the latter is the Husimi-lattice version of a water-like model similar to that proposed by Roberts and Debenedetti [14]. This can be easily deduced by comparing the original paper [14] with the tetrahedral cluster approximation developed in [18]. The square plaquettes of the Husimi lattice correspond to tetrahedral clusters on the bcc lattice, whereas plaquette orientations are related with the geometric structure of model molecules. Let us remark that, even though the current model neglects some details considered in [14] and [18] (namely, the distinction between donors and acceptors [14], and the presence of extra nonbonding configurations [14, 18]), it nonetheless reproduces the typical thermodynamic anomalies observed in real water. Such a result confirms that the physical mechanism underlying the anomalies is mainly based on the “weakening parameter” c , which favors states characterized by a positive correlation between higher local entropy (weaker bonds) and higher local density [14, 18]. A standard statistical-mechanical argument [9] relates such a positive correlation to a negative thermal expansion coefficient, *i.e.*, to the onset of a density maximum.

The replica-symmetric (RS) solution. — According to the cavity method [25], in the RS assumption, the model can be solved by a recursion equation for so-called “cavity biases” or “messages”. An elementary message $m_x^{a \rightarrow i}$ represents the probability of the x configuration at the i site, when the latter is detached from all plaquettes except a . With reference to fig. 1, denoting by \hat{m}_x the message from the central plaquette to the bottom site, the recursion equation reads

$$\hat{m}_x = e^f \sum_{x_1=0}^2 \sum_{x_2=0}^2 \sum_{x_3=0}^2 e^{-\beta h_{x,x_1,x_2,x_3}} \prod_{i=1}^3 \prod_{a=1}^3 m_{x_i}^{a \rightarrow i}, \quad (4)$$

where $\beta = 1/k_B T$ is the inverse temperature and f is a normalization constant, ensuring that $\sum_{x=0}^2 \hat{m}_x = 1$. Let us note that, in our case, since the lattice has no local heterogeneities, the messages do not depend on the position (one can drop the $a \rightarrow i$ superscript). Therefore, eq. (4) eventually simplifies to a set of three equations ($x = 0, 1, 2$) of the fixed-point form

$$m_x \propto \sum_{x_1=0}^2 \sum_{x_2=0}^2 \sum_{x_3=0}^2 e^{-\beta h_{x,x_1,x_2,x_3}} \prod_{i=1}^3 m_{x_i}^3, \quad (5)$$

where we have omitted the trivial normalization constant. These equations can be solved numerically by simple iteration. The actual probability p_x of the x configuration can

then be evaluated by considering the operation of attaching four equivalent branches, like that depicted in fig. 1, to the same “root” site [24]. One obtains $p_x \propto m_x^4$, where we have again omitted a normalization constant, needed to ensure $\sum_{x=0}^2 p_x = 1$. The RS solution is always characterized by $p_1 = p_2$, *i.e.*, no preference between the two molecule configurations. The mass density ρ is simply related to the occupation probability $p_{\text{occ}} = 1 - p_0 = p_1 + p_2$ as $\rho = (M/v)p_{\text{occ}}$, where $M \approx 18$ g/mol is the molecular mass of water and v is the volume per site (which is an adjustable parameter of the model).

The grand-canonical free energy per site F/N (let F and N denote respectively the thermodynamic free-energy times β , and the number of lattice sites) can be evaluated as a function of the messages as [24]

$$\frac{F}{N} = -\ln \frac{\sum_{x_0=0}^2 \sum_{x_1=0}^2 \sum_{x_2=0}^2 \sum_{x_3=0}^2 e^{-\beta h_{x_0, x_1, x_2, x_3}} \prod_{i=0}^3 m_{x_i}^3}{\left(\sum_{x=0}^2 m_x^4 \right)^3}. \quad (6)$$

Pressure can then be computed as $P = -(k_B T/v)(F/N)$. In the presence of multiple solutions of eq. (5), *i.e.*, of competing phases, the thermodynamically stable one is selected by the lowest free-energy (highest pressure) value. In general, the knowledge of the cavity biases allows one to compute all the thermodynamic properties of interest, including response functions, such as the specific heat, the isothermal compressibility $\kappa_T = (\partial \ln \rho / \partial P)_T$, and the isobaric thermal expansion coefficient $\alpha_P = -(\partial \ln \rho / \partial T)_P$, whose anomalous behavior is specially relevant in real water. It is also possible to obtain numerically simple equations for the loci of divergence of the response functions (spinodals) and the temperature of maximum density (TMD) locus at constant pressure, defined by $\alpha_P = 0$.

A fitting procedure has been performed to fix the model parameters. The hydrogen bond energy η and the volume per site v are easily computed as a function of the van der Waals energy ϵ and the weakening parameter c , by requiring the maximum density at 1 atm to be 1 g/cm³ and to occur exactly at 3.984 °C [28]. We have then fitted only the two parameters ϵ and c by minimizing (in a least-square sense)¹ the difference between a set of experimental density values at 1 atm (fig. 2, inset) and the corresponding theoretical values. The final result is: $\eta \approx 7.786$ kJ/mol, $\epsilon \approx 3.621$ kJ/mol, $c \approx 0.6450$, $v \approx 15.70$ cm³/mol.

In fig. 2 we report the RS phase diagram in the temperature-density plane. We obtain a quite good agreement with experimental data for the whole liquid-vapor binodal curve (not fitted). The critical exponent is not correct, due to the mean-field nature of the model, but the critical density $\rho_c \approx 0.3417$ g/cm³ is remarkably close to the experimental value 0.322 g/cm³ [28]. The TMD locus correctly displays a negative slope, quantitatively similar

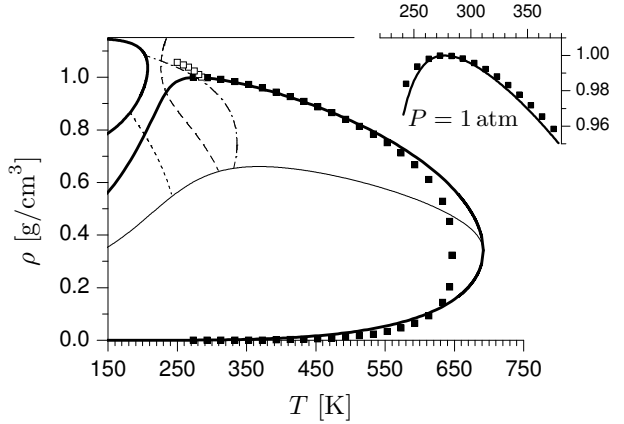


Fig. 2: Temperature-density phase diagram in the RS assumption. Thick solid lines denote binodals. Thin lines are defined by the following conventions: A solid line denotes the liquid spinodal, a dash-dotted line denotes the TMD locus, a dashed line denotes the stability limit of the RS solution, and a dotted line denotes the zero-entropy locus. Solid and open squares denote experimental results for the liquid-vapor binodal [29] and the TMD locus [30] (the latter data refer indeed to heavy water; pressure values have been converted to density values by [29]). The inset displays the isobar at $P = 1$ atm, along with the experimental values [28] used for parameter fitting.

to the experimental one. Moreover, in the metastable region of the liquid phase at very low densities (negative pressures), the TMD locus exhibits a slight reentrance (*i.e.*, positive slope), which has been predicted by simulations with various intermolecular potentials [31, 32]. At odd with such simulations, our TMD line eventually meets the spinodal line. In the pressure-temperature diagram, the two curves meet tangentially at a pressure minimum, as required for thermodynamic consistency [33], but the spinodal is not found to re-enter the positive pressure region. The latter fact contradicts Speedy’s early conjecture [34] about the divergent-like behavior of response functions in the supercooled liquid regime. Conversely, our model seems to support Stanley’s conjecture, as it predicts, at very low temperature, a “second critical point”, terminating a coexistence region of two different liquid-like phases. Unfortunately, all this coexistence region lies below the stability limit of the RS solution (dashed line in fig. 2), where the latter is no longer valid. The inadequacy of such a solution in this regime is also pointed out by the fact that its entropy becomes negative below a given temperature (dotted line in fig. 2).

Fig. 3 displays the isobaric specific heat and the isothermal compressibility as a function of temperature, at atmospheric pressure. The well-known anomalous behavior of these response functions, related respectively to entropy and density fluctuations [9], is reproduced by the model in a qualitatively correct fashion. This result is achieved without the singularity required by Speedy’s conjecture. Indeed, upon decreasing temperature, the theoretical curves do not exhibit any divergence, but only

¹We have used the MATLAB routine `lsqnonlin`.

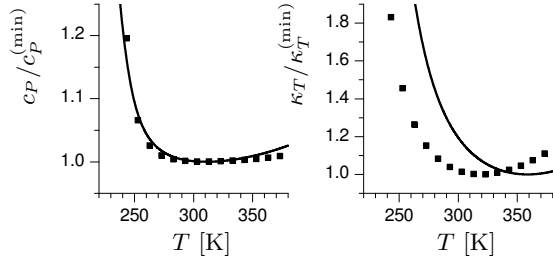


Fig. 3: Normalized isobaric specific heat (left) and isothermal compressibility (right) as a function of temperature at $P = 1$ atm. Lines and symbols denote respectively theoretical and experimental [28] results. The theoretical (experimental) minima occur at 37.45°C (36°C) and 85.58°C (46.5°C).

pronounced maxima. Quantitative agreement with experiments is not so good in this case, so that we report data normalized to the minimum values $c_P^{(\min)}$ and $\kappa_T^{(\min)}$.

The glassy phases. – Let us now investigate what happens when the RS ansatz does not hold. We make use of the cavity method at the level equivalent to 1-step replica symmetry breaking (RSB) [25]. For a given free-energy landscape, the complexity function $\Sigma(F)$ is defined as the log-number of minima (“pure states”, or simply “states”) with free energy in the range $[F, F + dF]$. If the number of states is exponentially large, then Σ is an extensive quantity. One can define a pseudo free-energy (“replicated” free-energy) as [35]

$$\Phi(\psi) = -\ln \sum_{\alpha} e^{-\psi F_{\alpha}}, \quad (7)$$

where F_{α} is the free energy of the α state, the sum runs over all states, and ψ is a pseudo inverse-temperature (Parisi parameter). A saddle-point calculation shows that $\Phi(\psi)$ is the Legendre transform of $\Sigma(F)$, so that $\Phi(\psi)$ allows one to reconstruct $\Sigma(F)$ via the parametric representation

$$F(\psi) = \frac{d\Phi}{d\psi}(\psi), \quad \Sigma(\psi) = \psi \frac{d\Phi}{d\psi}(\psi) - \Phi(\psi). \quad (8)$$

The replicated free-energy (and all the thermodynamic quantities) can be computed, as a function of ψ , by solving an integral equation for the message distribution² $\mathcal{P}(m)$ over the states

$$\mathcal{P}(m) = e^{\phi} \int \delta(m - \hat{m}) e^{-\psi f} \prod_{i=1}^3 \prod_{a=1}^3 \mathcal{P}(m^{a \rightarrow i}) dm^{a \rightarrow i}, \quad (9)$$

where both \hat{m} and f are defined by eq. (4) as functions of the set of incoming messages $\{m^{a \rightarrow i}\}$, and ϕ ensures the normalization condition $\int \mathcal{P}(m) dm = 1$. Equation (9) can be solved numerically by a population dynamics technique [25].

²Hereafter, m without subscript denotes a normalized 3-component array (m_0, m_1, m_2) .

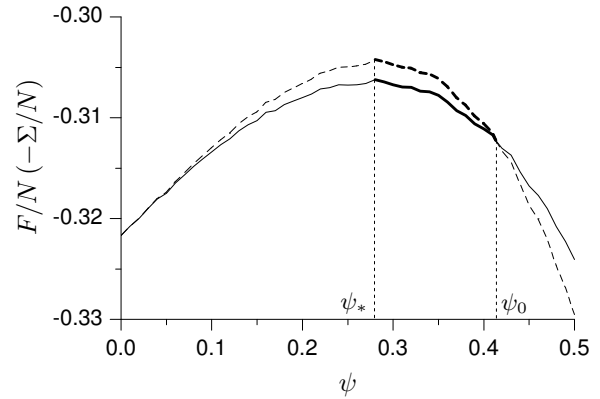


Fig. 4: F/N (dashed line) and $(F - \Sigma)/N$ (solid line) as a function of ψ at $T = 135$ K, $\mu/\eta = -2.38$. Thinner lines denote unphysical parts of the curves.

In the RS phase, $\mathcal{P}(m)$ is a delta-function and eq. (4) is recovered. The stability limit of the RS phase, displayed in fig. 2, can be determined by assuming that $\mathcal{P}(m)$ has only a slight variance around the RS value. One obtains a linearized “propagation equation” for the covariance matrix of $\mathcal{P}(m)$

$$\langle \delta m_x \delta m_y \rangle = \sum_{x'=0}^2 \sum_{y'=0}^2 K_{x,y;x',y'} \langle \delta m_{x'} \delta m_{y'} \rangle, \quad (10)$$

where the (9×9) “transfer matrix” is

$$K_{x,y;x',y'} = \sum_{i=1}^3 \sum_{a=1}^3 \frac{\partial \hat{m}_x}{\partial m_{x'}^{a \rightarrow i}} \frac{\partial \hat{m}_y}{\partial m_{y'}^{a \rightarrow i}}, \quad (11)$$

and the Jacobians $\partial \hat{m}_x / \partial m_{x'}^{a \rightarrow i}$ can be evaluated from eq. (4). The RS solution becomes unstable when the maximum eigenvalue of the transfer matrix (11) becomes larger than 1.

In the RSB phase, the thermodynamically relevant states are identified by a minimum (wrt ψ) of the function $F - \Sigma$, which properly takes into account that the probability measure may be split over a large number of states with free energy around F . We report the typical behavior of F/N and $(F - \Sigma)/N$ in fig. 4. The leftmost part of the curves ($\psi < \psi_*$) is unphysical, because $dF/d\psi = d^2\Phi/d\psi^2 < 0$, which is inconsistent with eq. (7). The rightmost part ($\psi > \psi_0$) is also unphysical, because $\Sigma < 0$. Therefore, the physical minimum of $F - \Sigma$ is attained at the crossing point ψ_0 , such that $\Sigma(\psi_0) = 0$. In the jargon of replica theory, this is called a “condensed” glass phase. The number of thermodynamically relevant states is sub-exponential, but there exists an exponentially large number of metastable states. Fig. 5 shows that the former states exhibit the largest density, $\rho(\psi_0)$, whereas the latter span a range of smaller density values, $\rho(\psi_*) < \rho < \rho(\psi_0)$.

Upon increasing temperature, we observe that the RSB phase undergoes a *continuous* transition to the RS phase,

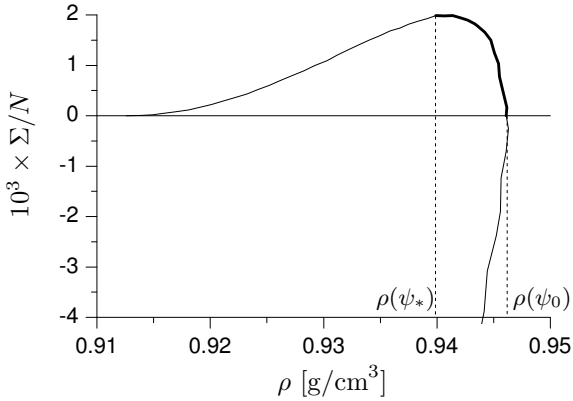


Fig. 5: Parametric plot of $\Sigma(\psi)/N$ vs. $\rho(\psi)$ at $T = 135$ K, $\mu/\eta = -2.38$ (as in fig. 4). Thinner lines denote unphysical parts of the curve.

at odd with the glass models cited above [1–5]. As previously mentioned, those models predict (upon *decreasing* temperature) an abrupt appearance of many metastable states (“dynamical transition”), where the system is expected to get stuck during quenching. Such a difference is rather intriguing. In real water, the glass transition appears to be much “weaker” than that found in the usual molecular liquids [36], and the very existence of a glass transition in water (before recrystallization upon heating) has been much debated [37, 38]. This “weakness” is believed to reflect a greater ease for the system to explore its energy landscape, *i.e.*, a greater accessibility of the ideal glass state [36]. Qualitatively speaking, such a scenario might be consistent with the absence of a dynamical transition, as predicted by our model.

Let us also consider the RSB phase at constant temperature. Fig. 6 shows that, upon increasing the chemical potential, a higher density solution appears discontinuously. It turns out that even the latter is a condensed glass phase, in the previously explained sense. As previously mentioned, we find it natural to identify these phases with the LDA and HDA ices. Remarkably, the density range predicted by the RSB solution for LDA is consistent with experimental values, at odd with the low-density (unstable) RS solution. The behavior of HDA, as a function of the Parisi parameter ψ , is qualitatively similar to that of LDA, displayed in fig. 4. Nevertheless, the density values of the metastable states are *higher* than the density of the thermodynamically relevant states, *i.e.*, $\rho(\psi_*) > \rho(\psi_0)$ (the ρ - Σ plot is a mirror image of that of fig. 5). Such a result guarantees that, even in the region where both solutions exist, they are always separated by a density gap with no states. As a consequence, our model supports the picture of a real first-order-like LDA-HDA transition [6, 9], excluding the possibility of a smooth crossover, suggested by some experimental observations [39]. The transition pressure at $T = 135$ K turns out to be about 28.6 MPa, much lower than the experimental estimate (~ 200 MPa) [40], but the decreasing trend, upon increasing temperature, is

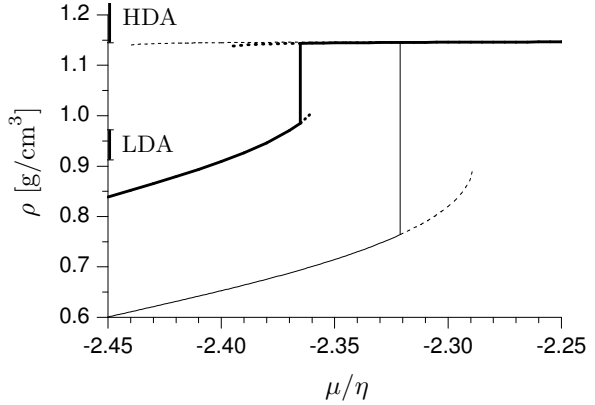


Fig. 6: Density ρ as a function of the normalized chemical potential μ/η at $T = 135$ K. Thinner lines denote the (unstable) RS solution; thicker lines denote $\rho(\psi_0)$ (*i.e.*, the density of the thermodynamically relevant states) in the RSB solution. Dotted lines denote metastable continuations. Experimental density ranges of LDA and HDA ices [40] are highlighted on the left axis.

correctly reproduced.

The transition line terminates in a critical point, which occurs around $T \approx 198$ K, $P \approx 16.7$ MPa, and above which the two glassy phases become indistinguishable. Note that, since LDA and HDA are, respectively, characterized by $\rho(\psi_*) < \rho(\psi_0)$ and $\rho(\psi_*) > \rho(\psi_0)$, indistinguishability implies $\rho(\psi_*) = \rho(\psi_0)$ in the supercritical region. This fact gives rise to a third kind of RSB phase (A), characterized by $\psi_0 = \psi_* = 0$ (see footnote³). The maximal complexity $\Sigma(\psi_*)$ of LDA and HDA turns out to vanish in a continuous way, defining two more (LDA-A and HDA-A) transition lines. Fig. 7 shows numerical evidence that such lines meet precisely at the critical point. The A-phase may still be considered a glassy phase, since the message distribution $\mathcal{P}(m)$ is still nontrivial. As previously mentioned, the vanishing complexity means that such a distribution represents a sub-exponential number of pure states. As shown in fig. 7, the A-phase region extends until the RS stability limit, where $\mathcal{P}(m)$ eventually degenerates into a Dirac delta, and the RS solution becomes stable.

Summary and conclusions. – We have studied a simplified model of water, defined on a Husimi lattice, which can be solved by the cavity method. Despite its simplicity, the model seems to capture a lot of features arising in real (and simulated) water, including thermodynamic anomalies of the liquid phase and a low-temperature glassy phase displaying polyamorphism. To the best of our knowledge, this is the first lattice model describing all these features together.

The glassy behavior originates in the competition between the tendency of the model to form regular hydrogen-bond networks, driven by the energy term $-\eta b_{x,y}$ of eq. (3), and the topological disorder of the Husimi lat-

³The corresponding complexity is $\Sigma = 0$; ψ values other than 0 result in a negative complexity.

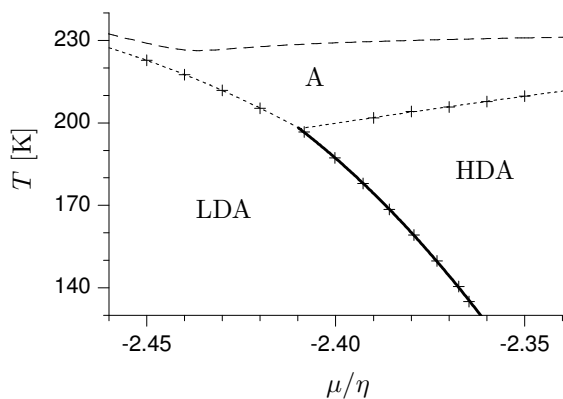


Fig. 7: RSB phase diagram (see the text). The dashed line denotes the RS stability limit. Other lines are 2nd order polynomial interpolations of symbols.

tice, which induces frustration. In other words, the lattice randomness plays a relevant role in the model behavior, as it is responsible for suppressing the ice-like phases that appear in the corresponding regular lattice models. Even though the latter feature might be considered a weakness of the model, we believe that it roughly illustrates the physical mechanism underlying glassy behavior in a hydrogen-bonded (network-forming) fluid. In this framework, the onset of polyamorphism is related to the fact that, due to the weakening term $+\eta b_{x,y}c(n_z + n_w)/2$, the original model predicts a low density network structure (stable at low pressure), besides the “ordinary” crystal-like ground state. The glass-glass transition may thus be viewed as a “frustrated” reminiscence of the coexistence between these two phases.

In the future, it might be interesting to investigate whether a similar mechanism could give rise to glass-glass transitions even for lattice models predicting a dynamical transition scenario [1–5]. A more technical issue, still deserving investigation, is the stability of the current picture with respect to further RSB steps.

REFERENCES

[1] FRANZ S., MÉZARD M., RICCI-TERSENGHI F., WEIGT M. and ZECCHINA R., *Europhys. Lett.*, **55** (2001) 465.
 [2] BIROLI G. and MÉZARD M., *Phys. Rev. Lett.*, **88** (2002) 025501.
 [3] PICA CIAMARRA M., TARZIA M., DE CANDIA A. and CONIGLIO A., *Phys. Rev. E*, **67** (2003) 057105.
 [4] WEIGT M. and HARTMANN A. K., *Europhys. Lett.*, **62** (2003) 533.
 [5] KRZAKALA F., TARZIA M. and ZDEBOROVÁ L., *Phys. Rev. Lett.*, **101** (2008) 165702.
 [6] LOERTING T. and GIOVAMBATTISTA N., *J. Phys.: Condens. Matter*, **18** (2006) R919.
 [7] MISHIMA O., CALVERT L. D. and WHALLEY E., *Nature*, **314** (1985) 76.
 [8] POOLE P. H., SCIORTINO F., ESSMANN U. and STANLEY H. E., *Nature*, **360** (1992) 324.

[9] DEBENEDETTI P. G., *J. Phys.: Condens. Matter*, **15** (2003) R1669.
 [10] BELL G. M., *J. Phys. C*, **5** (1972) 889.
 [11] LAVIS D. A. and SOUTHERN B. W., *J. Stat. Phys.*, **35** (1984) 489.
 [12] SASTRY S., SCIORTINO F., and STANLEY H. E., *J. Chem. Phys.*, **98** (1993) 9863.
 [13] BESSELING N. A. M. and LYKLEMA J., *J. Phys. Chem.*, **98** (1994) 11610.
 [14] ROBERTS C. J. and DEBENEDETTI P. G., *J. Chem. Phys.*, **105** (1996) 658.
 [15] SASTRY S., DEBENEDETTI P. G., SCIORTINO F. and STANLEY H. E., *Phys. Rev. E*, **53** (1996) 6144.
 [16] FRANZESE G. and STANLEY H. E., *J. Phys.: Condens. Matter*, **14** (2002) 2201.
 [17] FRANZESE G., MARQUÉS M. I. and STANLEY H. E., *Phys. Rev. E*, **67** (2003) 011103.
 [18] BUZANO C. and PRETTI M., *J. Chem. Phys.*, **121** (2004) 11856.
 [19] HENRIQUES V. B., GUISONI N., BARBOSA M. A. A., THIELO M. and BARBOSA M. C., *Mol. Phys.*, **103** (2005) 3001.
 [20] HØYE J. S. and LOMBA E., *Mol. Phys.*, **108** (2010) 51.
 [21] BUZANO C., DE STEFANIS E. and PRETTI M., *J. Chem. Phys.*, **129** (2008) 024506.
 [22] PRETTI M., BUZANO C. and DE STEFANIS E., *J. Chem. Phys.*, **131** (2009) 224508.
 [23] LAVIS D. A. and BELL G. M., *Statistical Mechanics of Lattice Systems*, Vol. 1 (Springer, Berlin) 1999, p. 173.
 [24] PRETTI M., *J. Stat. Phys.*, **111** (2003) 993.
 [25] MÉZARD M. and PARISI G., *Eur. Phys. J. B*, **20** (2001) 217.
 [26] MÉZARD M. and MONTANARI A., *J. Stat. Phys.*, **124** (2006) 1317.
 [27] CABANE B. and VUILLEUMIER R., *C. R. Geosci.*, **337** (2005) 159.
 [28] CHAPLIN M., <http://www1.lsbu.ac.uk/water/>.
 [29] LINSTROM P. J. and MALLARD W. G. (Editors), *NIST Chemistry WebBook, NIST Standard Reference Database Number 69* (National Institute of Standards and Technology, Gaithersburg MD, 20899) <http://webbook.nist.gov/>, retrieved November 21, 2008.
 [30] ANGELL C. A. and KANNO H., *Science*, **193** (1976) 1121.
 [31] NETZ P. A., STARR F. W., STANLEY H. E. and BARBOSA M. C., *J. Chem. Phys.*, **115** (2001) 344.
 [32] YAMADA M., MOSSA S., STANLEY H. E. and SCIORTINO F., *Phys. Rev. Lett.*, **88** (2002) 195701.
 [33] POOLE P. H., SCIORTINO F., ESSMANN U. and STANLEY H. E., *Phys. Rev. E*, **48** (1993) 3799.
 [34] SPEEDY R. J., *J. Phys. Chem.*, **86** (1982) 982.
 [35] MONASSON R., *Phys. Rev. Lett.*, **75** (1995) 2847.
 [36] ANGELL C. A., *Science*, **319** (2008) 582.
 [37] YUE Y. and ANGELL C. A., *Nature*, **427** (2004) 717; **435** (2005) E1.
 [38] KOHL I., BACHMANN L., MAYER E., HALLBRUCKER A. and LOERTING T., *Nature*, **435** (2005) E1.
 [39] TULK C. A. *et al.*, *Science*, **297** (2002) 1320.
 [40] MISHIMA O., *J. Chem. Phys.*, **100** (1994) 5910.